ELSEVIER

Thermochimica Acta 284 (1996) 67–83

thermochimica acta

Contributions of phase diagrams to the understanding of organized polymer–solvent systems[1]

Jean-Michel Guenet

Laboratoire d'Ultrasons et de Dynamique des Fluides Complexes, Université Louis Pasteur-CNRS URA 851, 4, RUE Blaise Pascal, F-67070 Strgasbourg Cedex, France

Abstract

When organized phases are formed in polymer–solvent systems through first-order transition, knowledge of the temperature–concentration phase diagram brings valuable information about their nature (polymer–solvent compound, peritectic, etc.), and also about the mechanisms involved during the organization process. The construction of these phase diagrams usually obeys Gibbs phase rules, even though formation often occurs under non-equilibrium conditions. In particular, the existence of invariants (monotectic transformations, peritectic, etc.) can still be observed. Knowledge of the phase diagram is also of prime importance for understanding rheological properties, particularly for thermoreversible gels. Examples dealing with these issues are given in this paper.

Keywords: Phase diagrams; Organized polymer–solvent systems; Non-equilibrium systems

1. Introduction

Until recently, investigations into the properties of crystallizable polymers were mainly carried out from the bulk state or from very dilute solutions, in the latter case for producing single crystals as perfect as possible [1]. Very few studies have been performed on polymer–solvent systems spanning the whole composition range. In these studies, it was unhesitatingly recognized that establishing the *temperature–concentration phase diagram* was an essential step if one were to gain understanding of

[1] Presented at the 24th North American Thermal Analysis Society Conference, San Francisco, CA, USA, 10–13 September 1995

0040-6031/96/$15.00 © 1996 – Elsevier Science B.V. All rights reserved
PII 0040-6031(96)02892-4

these systems [2]. For example, Carbonnel and Coworkers [3, 4] investigated polyester oligomers in a large variety of solvents. Smith and Pennings [5], and later Wittmann and St John Manley [6] studied the formation of eutectic solids consisting of a polymer and a high-melting solvent. Interest aroused by the occurrence of thermoreversible gelation synthetic polymers has given new consideration to the use of phase diagrams with polymer–solvent systems. As a matter of fact, polymer concentration is a very important parameter in the gelation phenomenon. To quote but one example, gelation is often said to proceed via or interfere with a spinodal decomposition, a phase separation mechanism restricted to the quenching of the solution into the miscibility gap. Knowledge of the phase diagram allows one to find out where this mechanism may take place. Also, the discovery of polymer–solvent compounds in different systems, including thermoreversible gels, is largely due to knowledge of their phase diagram [7–10].

The notion of the phase diagram implicitly conveys the concept of thermodynamic equilibrium. From a practical viewpoint, it can be stated that processes occurring under equilibrium conditions are independent of either the heating rate or the cooling rate, unlike those out of equilibrium. The question that immediately arises is: *to what extent can rules derived for equilibrium systems be applied unreservedly to systems formed far from equilibrium*?

In this paper, it will be shown that thermoreversible gels formed under non-equilibrium conditions can still be described using Gibbs phase results, and that the phase diagram can be an essential tool in accounting for their mechanical properties. Also, examples of phase diagrams for polymer–solvent systems formed under near-equilibrium conditions will be presented together with their impact on the knowledge of these systems.

2. Phase rules for systems at equilibrium

The most important feature in temperature–concentration phase diagrams for systems at equilibrium is the existence of *non-variant transformations*, that is transformations always occurring at the same temperature independent of the concentration. The existence of such transformations can be demonstrated through the *variance of the system*, a concept first established by Gibbs. The variance v_G is simply the number of parameters (temperature, concentration, etc.) that can be altered without modifying the equilibrium of the system. Determination of the variance is achieved by considering that for N components distributed in Φ phases in equilibrium, the chemical potential of one component is the same in all the phases

$$\begin{aligned} &\mu_A^\alpha = \mu_A^\beta = \mu_A^\gamma = ... \\ &\mu_B^\alpha = \mu_B^\beta = \mu_B^\gamma = ... \\ &\mu_C^\alpha = \mu_C^\beta = \mu_C^\gamma = ... \\ &..... \end{aligned} \tag{1}$$

There are, accordingly, $(\Phi - 1)$ independent equations for each component, and a total of $N(\Phi - 1)$ relations In addition, there are $\Phi(N - 1)$ independent variables related to concentrations of the components in all the phases. Taking into account pressure and temperature, the number of independent variables amounts to $2 + \Phi(N - 1)$.

The variance is then simply the number of independent variables minus the number of relations between them

$$v_G = N - \Phi + 2 \tag{2}$$

or at constant pressure, which is often the case with polymer–solvent systems

$$v_G = N - \Phi + 1 \tag{3}$$

The variance can also be regarded as the dimension of the locus delimiting the appearance of coexisting phases. Consider a system consisting of two components. If $\Phi = 1$, then $v_G = 2$, which means that a phase in equilibrium with itself on a *surface* (a two-dimensional object). If $\Phi = 2$, then $v_G = 1$, which implies that the locus is a *line* (a one-dimensional object). Finally, if $\Phi = 3$, then $v_G = 0$, and the locus reduces to a *point* (a zero-dimensional object).

This way of presenting the meaning of the variance allows one quite simply to account for the existence of *temperature-non variant transformations*. Fig. 1, in which two types of phase diagrams representing a eutectic system are drawn, provides one with an illustration of this statement. In the upper diagram of Fig. 1, the transformation

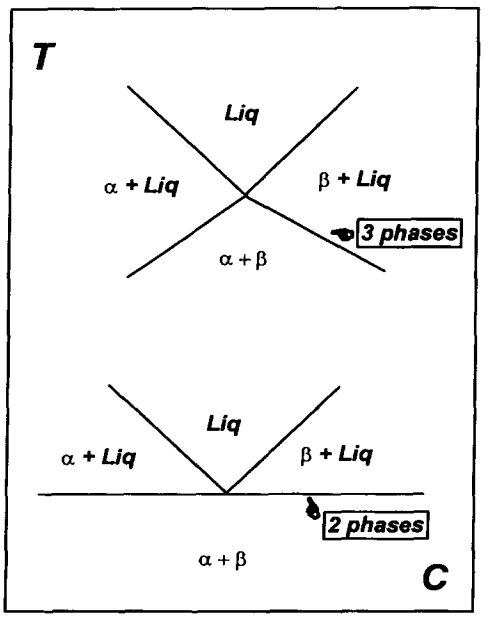

Fig. 1. Upper. A phase diagram not constructed following the Gibbs phase rule: 3 phases coexist on a line. Lower. Phase diagram complying to Gibbs phase rule: only two phases coexist on a line.

from $\alpha + \beta$ into β + liquid occurs on a line with no particular specifications. As a result, on this line three phases coexist: $\alpha + \beta$ + liquid, in conflict with the variance which specifies that only two phases should coexist on a line. The correct way to draw the phase diagram is shown in the lower diagram of Fig. 1. Here, the transformation from $\alpha + \beta$ into β + liquid occurs on a line at constant temperature. As a result, on this line only two phases coexist, in the present case β + liquid E (liquid of eutectic composition), which complies with the dimension given by the value of the variance.

Another important outcome from the theory of phase diagrams is *Tamman's plot* which predicts, through application of the *lever rule*, the variation of the enthalpy (or latent heat of fusion) associated with a first-order transformation as a function of concentration. Regrettably, this plot is seldom used or merely overlooked, although it provides valuable information. To illustrate its potentialities, consider, for instance, the non-variant eutectic melting represented in Fig. 2. For the eutectic composition C_e, there is only one melting endotherm corresponding to an enthalpyΔH_e. For other compositions, the enthalpy ΔH given off at the eutectic temperature is simply proportional to the mass fraction μ_e of the eutectic liquid formed, through the simple relation

$$\Delta H = \mu_e \times \Delta H_e \tag{4}$$

Enthalpies are expressed here in joules per gram of sample. If they were given in joules per mole, then μ_e would be the mole fraction instead. Thanks to the lever rule, μ_e can be

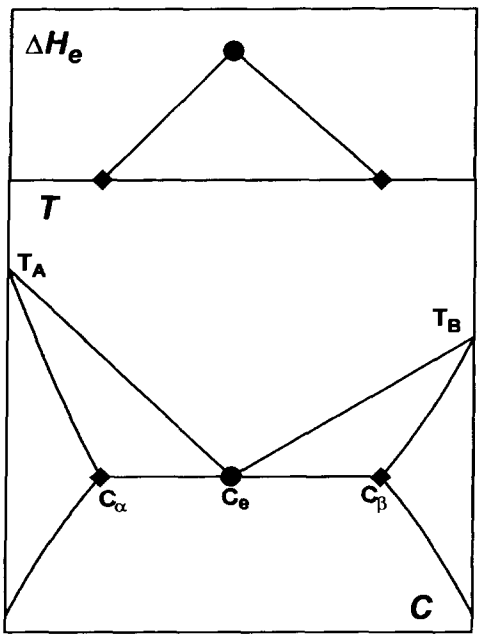

Fig. 2. Typical eutectic phase diagram. Tamman's plot represented above allows determination of C_α, C_β and C_e.

expressed straightforwardly through

$$\text{for} \quad C \leq C_e \quad \mu_e = \frac{C - C_\alpha}{C_e - C_\alpha} \tag{5}$$

$$\text{for} \quad C \geq C_e \quad \mu_e = \frac{C_\beta - C}{C_\beta - C_e} \tag{6}$$

in which C_α, C_β and C_e are the compositions of the α-phase, the β-phase and the eutectic liquid, respectively, and C the global concentration.

Relations (4), (5) and (6) indicate that: (i) the variation of ΔH with global concentration must be linear; and (ii) going from α to β, ΔH must increase from zero at $C = C_\alpha$ up to ΔH_e at $C = C_e$, and then decrease down to zero at $C = C_\beta$. Accordingly, C_α, C_β and C_e can all be determined quite straightforwardly by means of Tamman's plot.

In the case of polymer–solvent compounds, Tamman's plot allows determination of the compound stoichiometry.

3. Polymer–solvent systems formed far from equilibrium

3.1. A hypothetical case

The crystallization rate of many polymers turns out to be slow enough to permit the cooling of a polymer–solvent mixture well below the liquidus line, *i.e.* to high undercoolings ΔT, without spontaneous formation of crystals. Because of this property, the solution can undergo new type of phase separation otherwise forbidden. A typical example is the *monotectic transformation* which occurs when a liquidus line crosses a miscibility gap (see Fig. 3). The reaction at the monotectic line is therefore

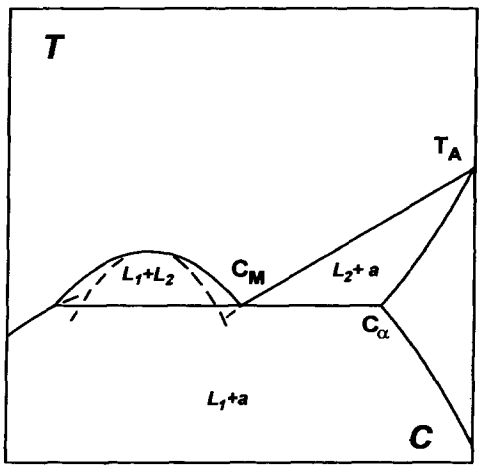

Fig. 3. Schematic representation of a monotectic transition. The dotted line represents the spinodal curve. Under the spinodal and under the binodal on the right-hand side of the miscibility gap, liquid–liquid phase separation must occur prior to crystallization.

α + liquid$_1$ α + liquid$_2$, in which liquid$_2$ possesses a higher polymer concentration than liquid$_1$. Now, in the case where a given polymer–solvent mixture could reach a miscibility gap for reasons given above, how would the phase diagram recorded on heating look? Would it show the features of equilibrium phase diagrams or look utterly different and unpredictable? To answer this question, a hypothetical situation depicted in Fig. 4 and an experimental result drawn in Fig. 5 will be considered.

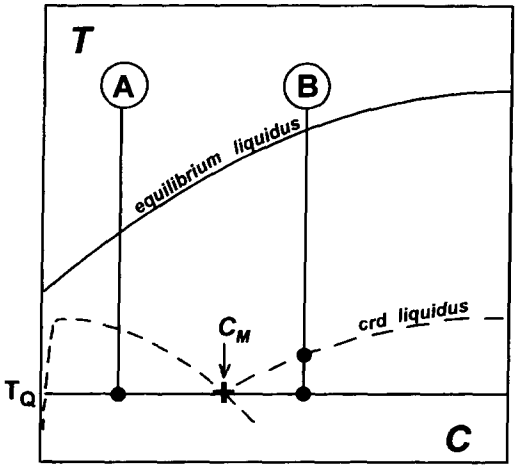

Fig. 4. Hypothetical diagram when rapid cooling rates are used and the system always quenched at T_Q. For details see text.

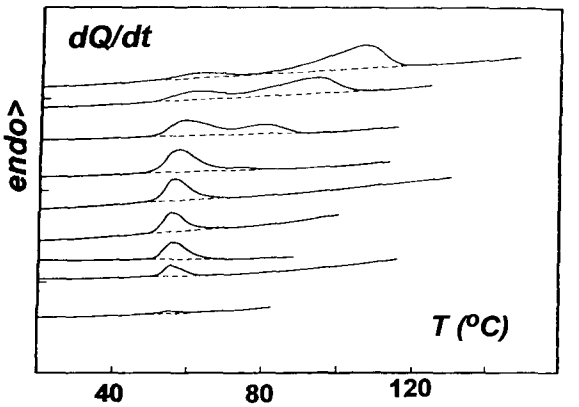

Fig. 5. Typical melting endotherms recorded at 20°C min^{-1} for thermoreversible gels obtained with a multiblock copolymer in *trans*-decalin. As can be seen, the low-melting endotherm is a non-variant transformation. Concentrations (% in w/w) from bottom to top: C_{pol} = 1.87, 5.45, 9.45, 11, 14.5, 19.6, 31.3, 41.3, 51.9.

Fig. 4 displays a case where the miscibility gap is well below the equilibrium liquidus line. Due to the slow crystallization kinetics, another liquidus line has to be considered. Its position will depend both upon the cooling rate and the temperature of quench, hence it designation as a cooling-rate-dependent liquidus (crd liquidus for short). Two typical cases deserve discussion: case A, $C < C_M$; and case B, $C > C_M$.

Case A

Here the solution is quenched within the miscibility gap. Under these conditions, Cahn has shown [11], by means of thermodynamic arguments, that in most of this domain liquid–liquid phase separation must occur prior to crystallization. As a result, the system will separate first into two liquids, a *polymer-poor liquid and polymer-rich liquid*, always with the same composition, independent of the starting concentration. The polymer in the polymer-rich phase will then crystallize giving crystals of identical melting point in a large range of polymer concentrations, since this takes place as if the different solutions were of the same concentration, i.e. C_M Consequently, one expects a non-variant melting point.

Case B

Here the solution first crosses the crd liquidus line and begins to form crystals. Continuous cooling to the quenching temperature T_Q gradually yields two phases: the *crystal phase* and a *liquid* whose composition will reach C_M at the quenching temperature. At this point the composition of this phase will no longer vary, since further dilution would give liquid–liquid phase separation which, in turn, would result in a phase composition C_M. This phase, once at C_M, will eventually undergo crystallization. Here, the same situation as described for case *A* prevails, so that crystals formed from this phase will have the same melting point independent of the starting concentration. Conversely, those formed directly from the crystal phase will possess a melting point which will increase with increasing polymer concentration.

The net result will be a non-variant melting point in all the range of concentrations and the appearance of a concentration-dependent melting point for concentrations higher than C_M. In the end, the melting phase diagram should look much the same as that obtained for equilibrium monotectic transformation, except that the monotectic line will be well above the miscibility gap.

3.2. *An experimental monotectic transformation*

Such a hypothetical case can actually be found experimentally for thermoreversible gels prepared from a multiblock copolymer constituted of crystallizable sequence alternating with non-crystallizable ones (further details on this system can be found in Refs. [12–14]). In Fig. 5, where the thermograms obtained with the system copolymer/*trans*-decalin are drawn, a non-variant transformation at $T_M = 55°C$ can be seen. This transformation ranges from $C \approx 0$ to $C = 0.56$, while another melting line increasing with copolymer concentration can be observed for concentrations larger than $C = 0.18$. The corresponding phase diagram is displayed in Fig. 6. Tamman's plot gives the value of C_M as well as C_α, the latter being the concentration of the solid

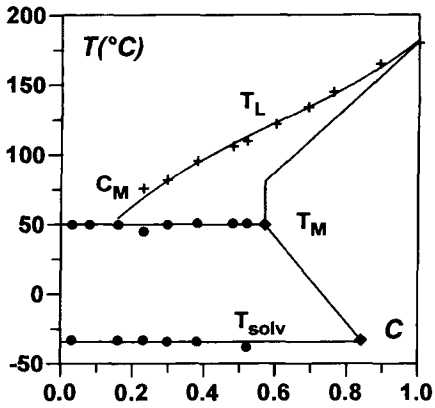

Fig. 6. Temperature–Concentration phase diagram for thermoreversible gels obtained with a multiblock copolymer (20% w/w of crystallizable sequence) in *trans*-decalin. T_{solv} represents the melting temperature of the crystallized solvent.

solution at T_M. Using turbidimetry experiments performed by cooling solutions of another copolymer sample of higher crystalline sequence content, the existence of a miscibility gap has been revealed [13]. This is presented in Fig. 7, where the monotectic and the liquidus lines as determined on heating are seen to be located well above the miscibility gap.

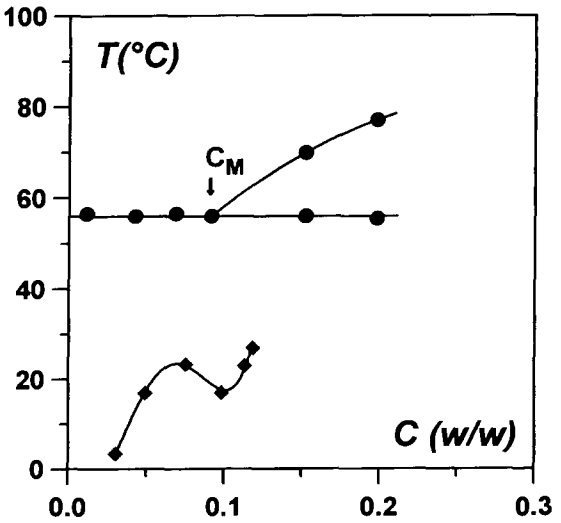

Fig. 7. Temperature–concentration phase diagram for thermoreversible gels obtained with a multiblock copolymer (50% w/w of crystallizable sequence) in *trans*-decalin. The lower curve (miscibility gap) was determined by turbidimetry at a 10°C min^{-1} cooling rate. As can be seen, the melting lines are well above the miscibility gap.

Interestingly, the evolution of the elastic modulus of these gels as a function of temperature, can be accounted for through knowledge of the phase diagram [12]. It is known that these gels possess a fibre-like morphology [12]. Partial melting of the crystalline junctions is equivalent to altering the "functionality" of the network. Here the functionality is taken as the number of fibres merging at the same junction. Jones and Marques [15] have shown that if the functionality is modified then the modulus should vary as the volume fraction of the network

$$E \simeq \varphi_N \tag{7}$$

Approximating φ_N to the fraction of polymer-rich phase, which is the phase constituting the network, and applying the lever rule gives the following relations

$$\varphi_N \simeq \frac{C_{prep}}{C_\alpha} \quad \text{for } T < T_M \tag{8}$$

$$\varphi_N = 0 \quad \text{for } C < C_M, \quad \text{for } T > T_M \tag{9}$$

$$\varphi_N \simeq \frac{C_{prep} - C_{Ml}(T)}{C_{\alpha s}(T) - C_{Ml}(T)} \quad \text{for } C > C_M, \quad \text{for } T > T_M \tag{10}$$

in which C_{prep} is the starting polymer concentration, and $C_{Ml}(T)$ and $C_{\alpha s}(T)$ the concentrations at a given temperature defined by the liquidus and the solidus lines, respectively.

It is convenient to plot the ratio of the modulus as measured at 20°C over the modulus determined at T to eliminate the proportionality constant. Fig. 8 shows that this simple approach, together with the support of the phase diagram, allows one to account quite satisfactorily for the experimental variation of the elastic modulus as a function of temperature.

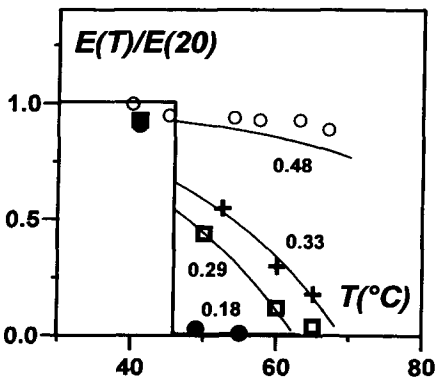

Fig. 8. Variation of the elastic modulus (plotted as the ratio of the modulus at T over the modulus at 20°C) as a function of temperature. The results can be fitted with the equations given in the text. Concentrations in w/w as indicated.

3.3. Other cases

Processes other than the liquid–liquid phase separation can be brought about by monitoring the cooling procedure. A typical example is given by isotactic polystyrene (iPS) in *cis*-decalin and in *trans*-decalin [9, 16, 17]. Depending on the quench temperature, phases with different molecular structures can be obtained. At low temperature (typically $T < 20°C$), a thermoreversible gel is formed. This phase is highly stable in that it does not evolve over a very long period of time (several years so far). Klein *et al.* [16] have shown that gelation occurs at a very well-defined temperature, T_{gel}; if the solution is quenched to below T_{gel}, then whatever the gelation kinetics, only a gel is formed (actually the kinetics becomes exceedingly slow when approaching from below the gelation threshold). It has been shown that the phase diagrams are different for *cis*-decalin and *trans*-decalin [9]. In both cases polymer–solvent compounds are formed but with differing stoichiometries: 1.15 *cis*-decalin/monomer and 1.75 *trans*-decalin/monomer. These stoichiometries throw light on why iPS/*trans*-decalin gels melt some 25°C higher than iPS/*cis*-decalin gels: the more solvated the compound, the lower its melting point.

It is worth emphasizing that phase diagrams first revealed the existence of polymer–solvent compounds in these systems. As a matter of fact, the molecular organization is so poor that diffraction methods proved to be of no avail [16–18].

Again the mechanical properties, if not quantitatively accountable, can be better understood through the availability of the phase diagram. Figure 9 is a double logarithmic plot which shows the variation of the elastic modulus as a function of polymer concentration for iPS/*trans*-decalin gels [19]. As can be seen, departure from linearity occurs at relatively low polymer concentrations. Bearing in mind that

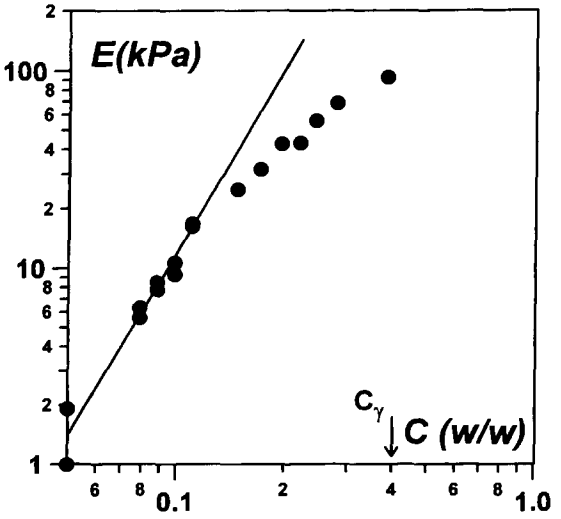

Fig. 9. Variation of the isochronal modulus as a function of polymer concentration (in g cm^{-3}) represented in a double logarithmic scale. C_γ stands for the stoichiometric concentration.

a compound behaves as a pure substance, one should rescale the values of concentrations, since a 40% polymer concentration for this system (stoichiometric concentration) corresponds in fact to a 100% compound concentration. As one does not expect power laws for modulus–concentration relations to hold for concentrations up to 100%, it is not surprising that departure from linearity is seen on approaching the stoichiometric concentration.

Just above the gelation temperature spherulitic structures grow, as opposed to fibrillar structures below. In the case of iPS/*trans*-decalin, these spherulites are constituted of the usual chain-folded crystals. Couversely, in the case of iPS *cis*-decalin, there are three varieties of stable phases in addition to the gel phase: the *s-phase*, formed just above the gel phase, the *p-phase* formed above the s-phase, and finally the *crystalline phase* [17]. The appearance of these different phases depends on the quenching temperature. Typical DSC traces of the s-phase and the p-phase are given in Fig. 10. The phase diagrams obtained on melting for the s-phase and the p-phase exhibit non-variant transformations (Figs. 11 and 12). These diagrams together with Tamman's plot (Fig. 11) suggest that the s-phase consist of a polymer–solvent compound of the same stoichiometry as that in the gel state but more organized at the molecular level [17]. The p-phase would consist of a pertitectic since the low-melting peak enthalpy shows a maximum as a function of polymer concentration (Fig. 12). At the corresponding temperature, the peritectic transforms into a liquid phase and a crystalline phase. Note that an incongruently-melting compound is a special case of peritectic [20]. In other words the p-phase is also some kind of compound. Here, there is an illustration of what has been claimed above, *i.e.* provided the system is quenched at always the same temperature, non-variant transformations can be observed. The peritectic transformation, although non-variant as a function of concentration is, however, significantly dependent upon the quench temperature (see Fig. 12).

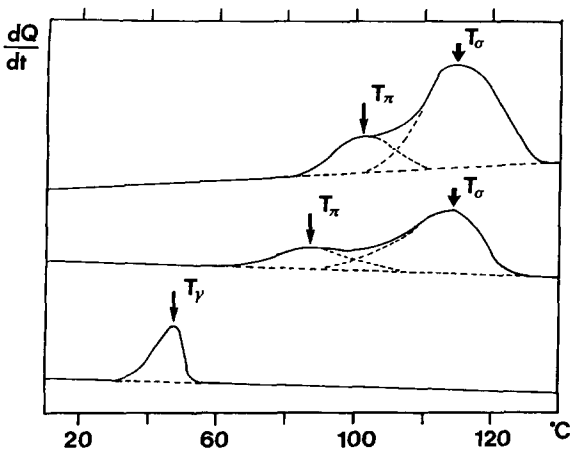

Fig. 10. Typical endotherms recorded for the p-phase and the s-phase. Lower curve, sample annealed at 25°C, middle curve, sample annealed at 45°C; and upper curve, sample annealed at 55°C.

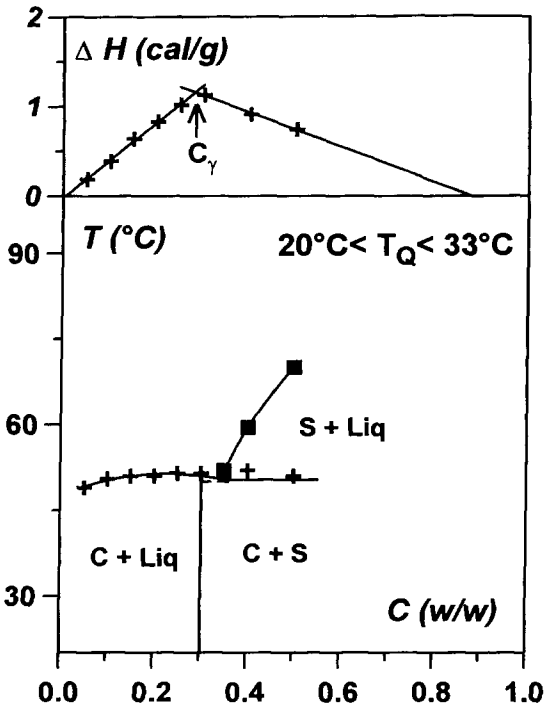

Fig. 11. Phase diagram of the s-phase. The melting always occurred at 52 ± 2°C independent of the quench temperature (from 21 to 31°C). This diagram is consistent with a congruently melting compound. Tamman's plot shows a maximum at $C = 0.3$ (w/w) which gives the same stoichiometry as in the gel state.

Structural studies give support to the deductions made from these diagrams (further details on the molecular structure can be found in Ref. [17]).

A formation phase diagram can be established (Fig. 13) that gives the T–C domains into which the solution must be quenched so as to produce these four different phases. Again, the Gibbs phase rule, and particularly the observation of non-variant transformations, holds here although the phases produced will be strongly dependent upon the quench temperature.

4. Polymer–solvent systems formed under equilibrium

Systems for which the phase diagrams obtained on cooling and on heating are similar can be regarded as being formed under equilibrium conditions. It is worth underlining that, due to the involvement of first-order transitions and the use of finite rates, there is usually a temperature shift between the diagram obtained on cooling and that determined on heating, the latter standing a few degrees above the former.

Here, two cases are discussed for which the phase diagram proved to be of invaluable support for the determination of the gelation mechanisms and the molecular structure.

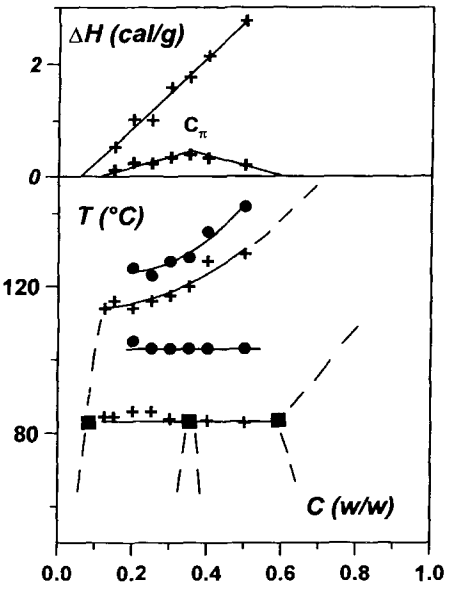

Fig. 12. Phase diagram of the p-phase. The low-melting endotherm is non-variant with concentration but depends upon the quench temperature. Typically, if the quench is achieved between 33 and 45°C, the non-variant transformation occurs at 85°C, whereas for higher temperatures this transformation is shifted to 100°C.

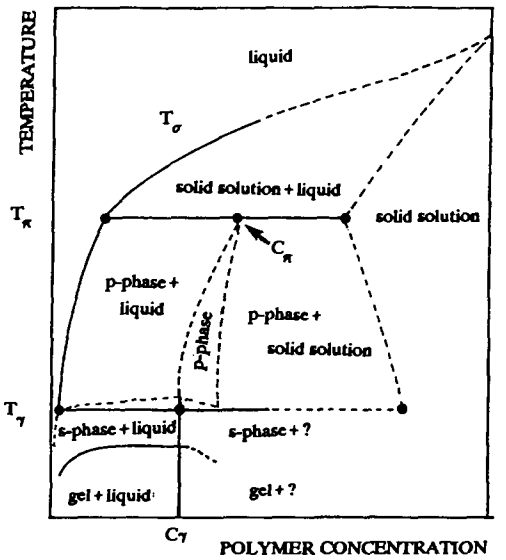

Fig. 13. Formation phase diagram summarizing the information gained from different quench temperatures.

4.1. *Atactic polystyrene/carbon disulphide gels (aPS/CS_2)*

The report on the themoreversible gelation of atactic polystyrene, a polymer not crystallizable from the melt, came as a surprise, or was simply not believed [21]. Attempts to explain the phenomenon took into account solvent quality as the key parameter CS_2; was regarded as a bad solvent, being capable of promoting polymer–polymer interactions and eventually some kind of aggregation/gelation [22]. It turns out that in the temperature domain where gelation occurs CS_2 is certainly not a bad solvent but, on the contrary, a good solvent [23, 24]. The tendency towards aggregration of aPS in good solvent was in fact known for years from light-scattering experiments but remained totally puzzling and unexplained [25–27]. The first hint as to the mechanism involved was given by the phase diagram. As a matter of fact, gelation of aPS gives off a latent heat which is but a first-order transition, implying that this process occurs through the formation of order, a fact later confirmed by diffraction techniques [28]. The phase diagram, together with Tamman's plot drawn in Fig. 14, are consistent with the existence of a polymer–solvent compound [10]. Also, the formation

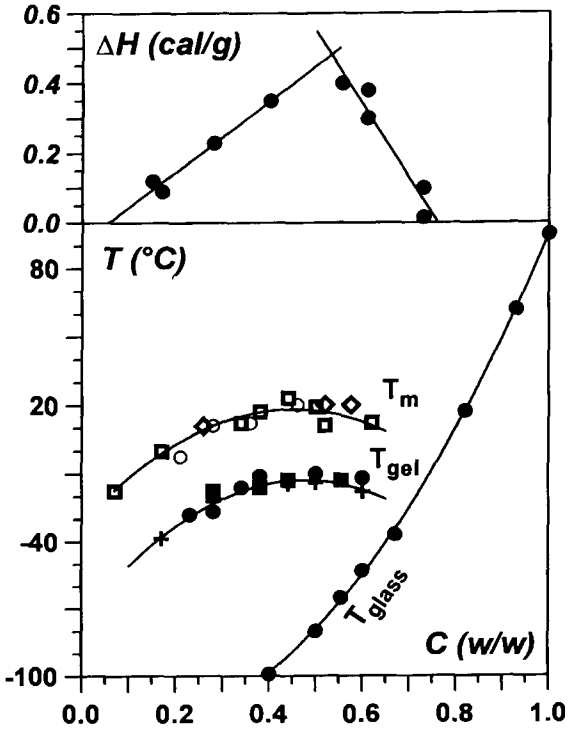

Fig. 14. Phase diagram for the gelling system atactic polystyrene/carbon disulphide (aPS/CS_2): T_m gel melting temperature; T_{gel} gel formation temperature; T_{glass} glass transition. Above, Tamman's plot. Here different molecular weights have been used (see reference [10] for further details)

diagram is similar to the melting diagram, but, as expected, shifted down by a few degrees. The existence of a polymer–solvent compound allows one to understand why aggregates of this polymer are often found in good solvents. Despite the common belief, a good solvent does not necessarily preclude crystallization, and, accordingly, the formation of a compound which requires affinity between polymer and solvent is more likely to occur in a good rather than in a bad solvent.

4.2. *Syndiotactic polystyrene/benzene (sPS/benzene)*

This system forms thermoreversible gels [29]. Whatever the cooling and heating rates used, sPS/benzene mixtures always give the same type of phases. This is illustrated by the thermograms recorded on heating/cooling exhibiting two endothermic/exothermic peaks (Fig. 15). The low-melting endotherm turns out to be a non-variant transformation occurring at $T \approx 76°C$, which is approximately the boiling point of benzene (DSC experiments were carried out in sealed pans). The phase diagram drawn in Fig. 16 is consistent with an incongruently melting compound [30]. Tamman's plot for the low-melting endotherm shows a maximum at $C_{pol} \leq 0.26$ (w/w) and reaches zero for $C_{pol} \leq 0.56$ (w/w). The maximum ought to correspond to the stoichiometry of this compound which yields approximately 4 benzene molecules per monomer unit. The vanishing of the low-melting endotherm could correspond either to a solid solution or to another compound. Neutron diffraction experiments definitely show that it is another compound [30]. The stoichiometry provided by Tamman's plot is therefore 1 benzene molecule per monomer unit.

Now only does the phase diagram allow determination of the stoichiometries of either compound but it also delivers another message: 3 out of 4 benzene molecules

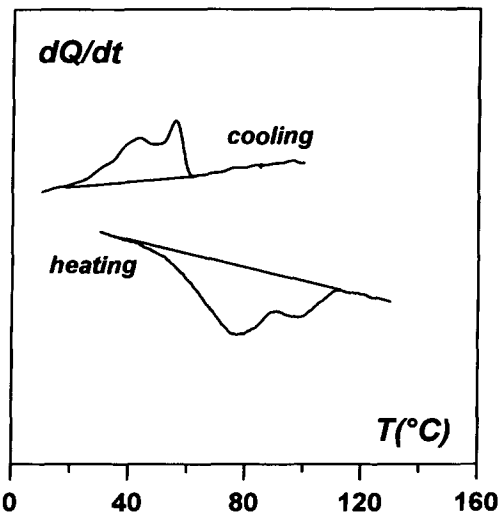

Fig. 15. Typical DSC traces obtained with the system SPS/benzene. The low-melting endotherm and the low-formation exotherm are both non-variant with concentration. $C = 25\%$ w/w.

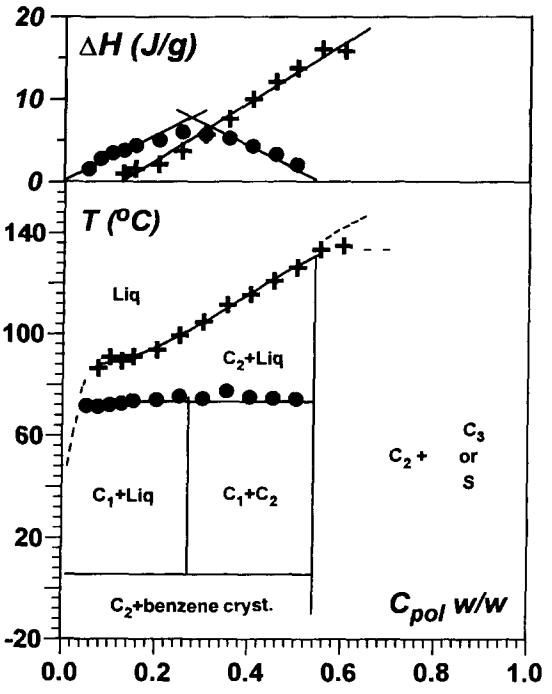

Fig. 16. Phase diagram and Tamman's plot for sPS/benzene gels.

involved in the first compound are very labile since incongruent melting takes place at benzene's boiling point, while one molecule is strongly bound. This led Daniel *et al.* [30] to put forward a molecular model in which one benzene molecule is housed between adjacent phenyl groups for a 2_1 helical structure. Under these conditions, the stoichiometry 1/1 is fulfilled and the interaction between benzene and polystyrene is thought to be strong enough to prevent the solvent molecule from being released at the boiling point of benzene. The diffraction pattern of the second compound can be accounted for by means of this molecular model.

Clearly without the help of the phase diagram the existence of the two compounds would not have been necessarily suspected, and diffraction experiments, especially those carried out for concentrations between 0.26 and 0.56, would have been totally misleading.

5. Concluding remarks

This paper is an attempt to stress that Gibbs phase rules can be used even in the case of systems formed under non-equilibrium conditions, provided that the rate of cooling and the quench temperature are kept constant for all concentrations. In any case, knowledge of the phase diagram is of prime importance to gain an understanding of the

systems under study. As a rule, the phase diagram should be the first thing established before investigating the system in more detail. Without the phase diagram, scientific discussion about an organized polymer–solvent system is meaningless.

References

[1] See, for example, Treatise on Solid State Chemistry ed. B. Hannay (Plenum Press) N.Y. 1967.
[2] R. Koningsveld, W.H. Stockmayer and E. Nies, Makromol. Fr. Chem. Macromol. Symp., 19 (1990) 1.
[3] L. Carbonnel, R. Guieu and J.C. Rosso, Bull. Soc. Chim. Fr., 8–9 (1970) 2855.
[4] J.C. Rosso, R. Guieu, C. Ponge, L. Carbonnel, Bull. Soc. Chim. Fr., 9–10 (1973) 2780.
[5] P.L. Smith, A.J. Pennings, Polymer, 15 (1974) 413.
[6] J.C. Wittmann, St John Manley, R. J. Pol. Sci. Polym. Phys. Ed., 15 (1977) 1089.
[7] J.J. Point, C. Coutelier, J. Pol. Sci. Polym. Phys. Ed., 22 (1984) 231.
[8] J.J. Point, P. Damman, Macromolecules, 25 (1992) 1184.
[9] J.M. Guenet, G.B. McKenna, Macromolecules, 21 (1988) 1752.
[10] J. François, Y. Gan, J.M. Guenet, Macromolecules, 19 (1986) 2755.
[11] J.W. Cahn, J. Am. Ceram. Soc., 52 (1969) 118.
[12] X.W. He, J. Herz, J.M. Guenet, Macromolecules, 20 (1987) 2003.
[13] X.W. He, J. Herz, J.M. Guenet, Macromolecules, 21 (1988) 1757.
[14] X. He, J. Herz, J.M. Guenet, Macromolecules, 22 (1989) 1390.
[15] J.L. Jones, C.M. Marques, J. Phys. (Les Ullis), 51 (1990) 1113.
[16] M. Klein, A. Menelle, A. Mathis, J.M. Guenet, Macromolecules, 23 (1990) 4591.
[17] J.M. Guenet, A. Menelle, V. Schaffhauser, P. Terech, A. Thierry, Coll. Polym. Sci., 272 (1994) 36.
[18] M. Girolamo, A. Keller, K. Miyasaka, N. Overbergh, J. Pol. Sci. Polym. Phys. Ed., 14 (1976) 39.
[19] G.B. McKenna, J.M. Guenet, J. Pol. Sci. Polym. Phys. Ed., 26 (1988) 267.
[20] A. Reisman, Phase Equilibria, Academic Press, New York, 1970.
[21] H. Tan, A. Hiltner, E. Moet, E. Baer, Macromolecules, 16 (1983) 28.
[22] R.F. Boyer, E. Baer, A. Hiltner, Macromolecules, 18 (1985) 427.
[23] M. Daoud, J.P. Cotton, B. Farnoux, G. Jannink, G. Sarma, H. Benoit, R. Duplessix, C. Picot, P.G. de Gennes, Macromolecules 8 (1975) 804.
[24] Y. Gan, A. Nuffer, J.M. Guenet, J. François, Polym. Commun., 27 (1986) 233.
[25] A.J. Hyde, R.B. Taylor, Makromol. Chem., 62 (1963) 204.
[26] H. Benoit, C. Picot, Pure Appl. Chem., 12 (1966) 545.
[27] Dautzenberg, Faserforsch. Textiltech., 21 (1970) 117.
[28] J.M. Guenet, M. Klein, A. Menelle, Macromolecules, 22 (1989) 494.
[29] M. Kobayashi, T. Nakaoki and T. Ishihara, Macromolecules, 23 (1990) 78.
[30] C. Daniel, M.D. DeLuca, A. Menelle, A. Brûlet, J.M. Guenet, Polymer, 37 (1996) 1273.